J Electroceram (2009) 23:121–126
DOI 10.1007/s10832-007-9323-z

Investigation of phase distribution in nanoscale $BaTiO_3$ powders prepared by hydro-thermal synthesis

S.-M. Moon · N.-H. Cho

Received: 31 May 2007 / Accepted: 30 August 2007 / Published online: 25 September 2007

Abstract Nanoscale $BaTiO_3$ powders were prepared by hydro-thermal synthesis; a mixture of H_2O and EtOH was used as solvent and the phase distribution of the powders was investigated in terms of the ratio (R) of DI water, H_2O/(H_2O+EtOH). The size of the powders was varied in the range of 20~100 nm depending on the solvent condition. X-ray diffraction and Raman spectroscopy were applied to investigate the variation in the relative volume fraction of the tetragonal phase; most of the powders contain both tetragonal and cubic phases. The results obtained by the two different analysis methods appear to be very close to each other, and it was found that the maximum volume fraction of the tetragonal phase was 23~26% when the synthesis was performed at R=0.25~0.5.

Keywords Nano-$BaTiO_3$ powder · Size control · Phase analysis

1 Introduction

Barium titanate ($BaTiO_3$) is one of the most popular ferroelectric materials with a perovskite structure. It has been widely used in various electronic devices like multi-layer capacitors, infrared detectors, fuel evaporators, varistors, and electro-optic devices for their unique and useful electrical characteristics. The electrical features of $BaTiO_3$ ceramics have been known to be crucially determined by the structural and chemical characteristics of the grains [1].

S.-M. Moon · N.-H. Cho (✉)
Department of Materials Science and Engineering,
Inha University,
Inchon 402-751, South Korea
e-mail: nhcho@inha.ac.kr

It has been known that $BaTiO_3$ has four different kinds of crystal structures like rhombohedral, orthorhombic, tetragonal, and cubic phases depending on temperature. In particular, its unit cell is of the cubic phase above Curie temperature (approximately 120°C); this cell has non-polar characteristics. Below the Curie temperature, the unit cell is slightly distorted to have the tetragonal phase; its dipole is parallel to its <001> direction [2]. However, some researchers have reported the effect of particle size on the room temperature structure of $BaTiO_3$; the cubic phase increases with decreasing particle size below approximately 1 μm [3].

Such size effect of $BaTiO_3$ ceramics is expected to play an important role in determining the crystal phase and dielectric properties of the powders in sub-micrometer size as well as nano-grained $BaTiO_3$ ceramics. Therefore, it is indispensable to obtain good understanding of how the phases of the nanoscale $BaTiO_3$ particles prepared via various synthesis routes are affected by synthesis methods and process variables [4, 5].

In this study, nanoscale $BaTiO_3$ powders were prepared by hydro-thermal synthesis as a function of synthesis solvent conditions. Their structural variation with synthesis variables was analyzed by X-ray diffraction, Raman spectroscopy and FT-IR. The shape and size change of the $BaTiO_3$ powders was examined, and these were related with the structural variation depending on the solvent conditions.

2 Experimental

Barium hydroxide octahydrate ($Ba(OH)_2 \cdot 8H_2O$) and titanium tetrachloride ($TiCl_4$) were used as source materials of Ba and Ti, respectively. CO_2-free deionized water was used in the preparation of all aqueous solutions to prevent contamination of barium based carbonates. Modification of titanium

tetrachloride was achieved by adding CO_2-free deionized water (ice-cold water) to prepare an aqueous 1 M $TiOCl_2$ stock solution; this is because $TiCl_4$ has large vapor pressure at room temperature and is readily hydrolyzed by reacting with water vapor in air. This aqueous $TiOCl_2$ stock solution was kept at its stable condition without being precipitated at room temperature. This stock solution was diluted to obtain a transparent aqueous $TiOCl_2$ solution with the Ti^{4+} concentration of 0.1 M for precipitation.

Amorphous titanium hydrous gel was prepared by adding NH_4OH into $TiOCl_2$ solution at 60°C for 2 h; this solution was stirred at 600 rpm during the process. After that, a raw material of Ba and Ti was introduced into a 40 $M\ell$ teflon-lined stainless steel vessel with a mixed solution of DI water and ethanol. The volume fraction (R) of DI water, $R=H_2O/(H_2O+EtOH)$, in the mixed solution was adjusted to be 1, 0.5, 0.25, 0.11, and 0, respectively. The sealed vessel was held at 180°C for 6 h. After cooling down to room temperature, the resultant precipitates were washed with water several times, and finally dried at 80°C for 12 h in an oven.

Their structural analysis were carried out by X-ray diffraction (XRD, Rigaku DMAX-2500), Raman spectroscopy (Bruker RFS100/S), and FT-IR (Shimadzu, IRPrestige-21); the shape and size distribution of the $BaTiO_3$ powders were examined by transmission electron microscopy (TEM, Philips CM200).

3 Results and discussion

Figure 1 show the bright-field TEM images of the nanoscale $BaTiO_3$ powders. The average size of the powders is about 100, 80, 50, 20, and 20 nm when R is 1, 0.5, 0.25, 0.11, and 0, respectively. The size of nanoscale $BaTiO_3$ powders was significantly dependent on the volume fraction of DI water in the solvent; it gradually decreased with increasing the ethanol fraction. This

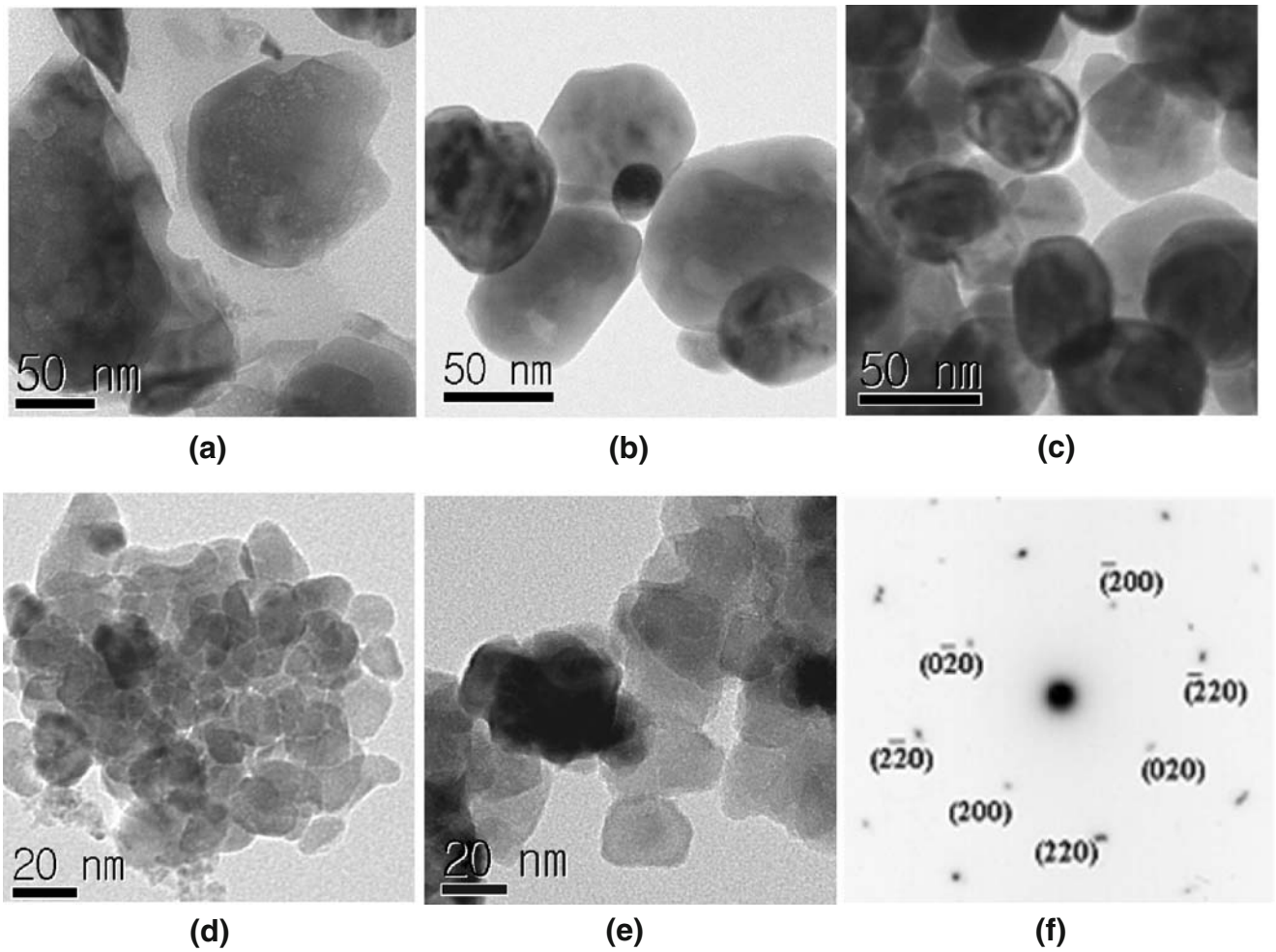

Fig. 1 Bright-field TEM images of the nanoscale $BaTiO_3$ powders. These powders were prepared by hydro-thermal synthesis at 180°C for 6 h at R=1(**a**), 0.5(**b**), 0.25(**c**), 0.11(**d**), and 0(**e**), respectively. (**f**) Selected area diffraction pattern (SADP). This pattern was recorded from one of the $BaTiO_3$ powders

indicates that the growth of nucleated $BaTiO_3$ powders is critically affected by ethanol fraction in the solvent.

In the dissolution-reprecipitation process, DI water is known to accelerate the dissolution of the precursor in the solution, which is beneficial to the formation of large particles [6]. The precursor is expected to have less solubility in an alcohol solution than that in water; this leads to the synthesis of smaller $BaTiO_3$ powders. The powders prepared at small R values appear to have a nearly sphere shape; however, when the size of the powders increases to be > ~80 nm, the surface tend to be parallel to crystallographic planes; in particular, in the powders prepared at R=0.5, facets parallel to (110), (40), and (10) planes are observed. A selected area diffraction pattern (SADP) in Fig. 1 (f) indicates that the powders are of a considerably high crystallinity.

The electron diffraction patterns from the samples prepared at R=0.25 and 0.11 are presented in Fig. 2 (a)

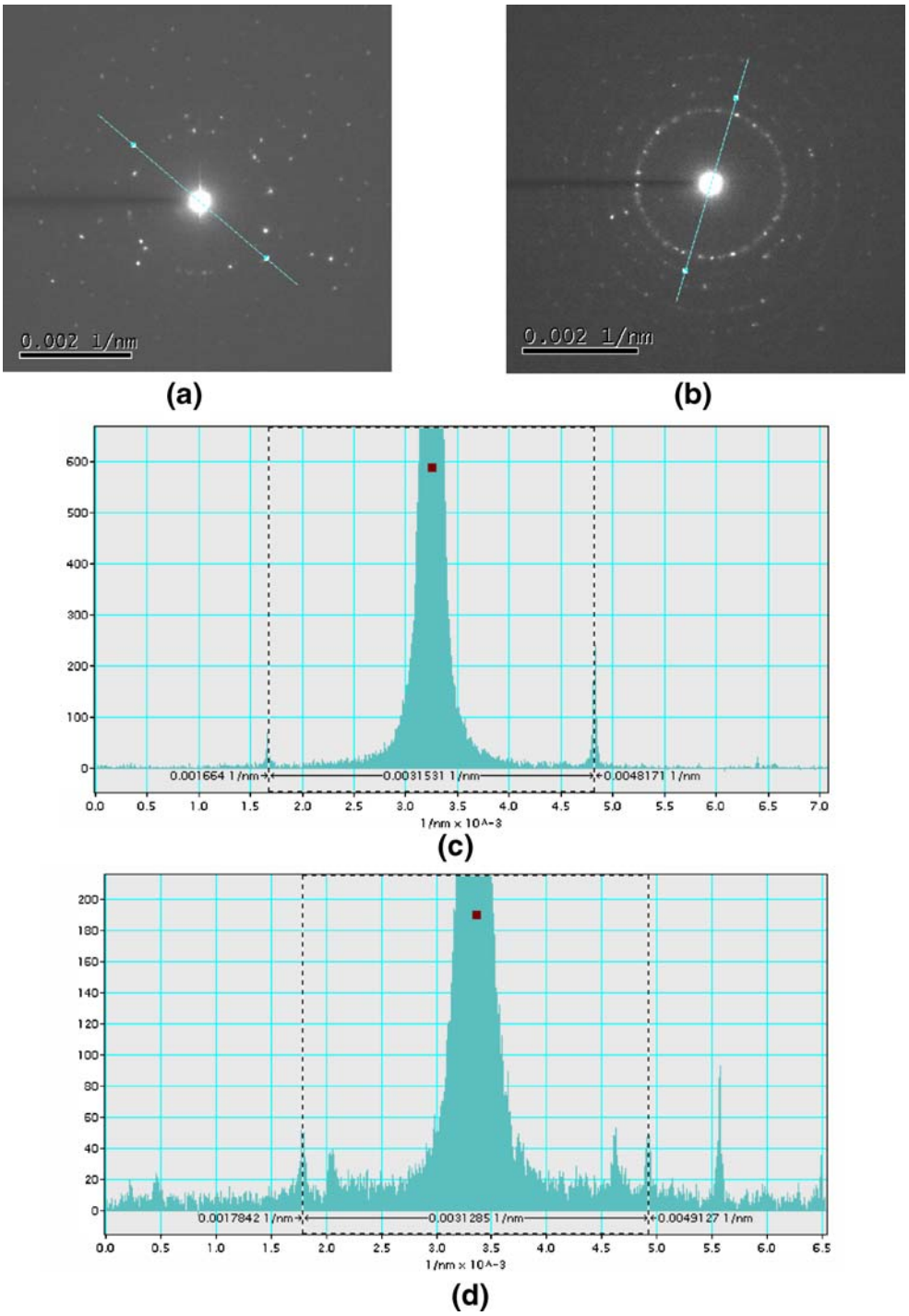

Fig. 2 (**a**) and (**b**) Electron diffraction patterns recorded from the powders prepared at R=0.25 and 0.11, respectively. (**c**) and (**d**) show intensity profiles along the lines seen in (**a**) and (**b**), respectively

and (b), respectively; these patterns were recorded at the same camera constant. The reciprocal spacing for (200) reflections was measured in the electron diffraction patterns [Fig. 2 (a) and (b)] using Gatan Digitalmicrograph. The (200) plane spacing was analyzed with a line-profile method; in this measurement, one pixel corresponds to 2.5×10^{-6} 1/nm. The (200) plane spacing is 1.58×10^{-3} 1/nm for the powders prepared at R=0.25, while 1.56×10^{-3} 1/nm for the samples synthesized at R=0.32 [Fig. 2 (c) and (d)]. As a result, the difference in the (200) plane spacing was determined to be 2×10^{-5} 1/nm; this value appears to be considerably larger than that of one pixel scale in the measurement and terms out to be ~0.23 Å in the real space. It seems highly likely that the value of 0.23 Å is related with the difference in the lattice parameter between the cubic and the tetragonal phases.

Figure 3 shows the XRD results of the $BaTiO_3$ powders. Diffraction peaks were observed at positions corresponding to the meta-stable cubic phase. Such a stabilization is known to be common in hydro-thermally synthesized $BaTiO_3$ powders, and this is explained by the entrapment of hydroxyl groups in the perovskite lattice.

When the size of $BaTiO_3$ powders is below ~1 μm, the full-width at half-maximum (FWHM) of corresponding

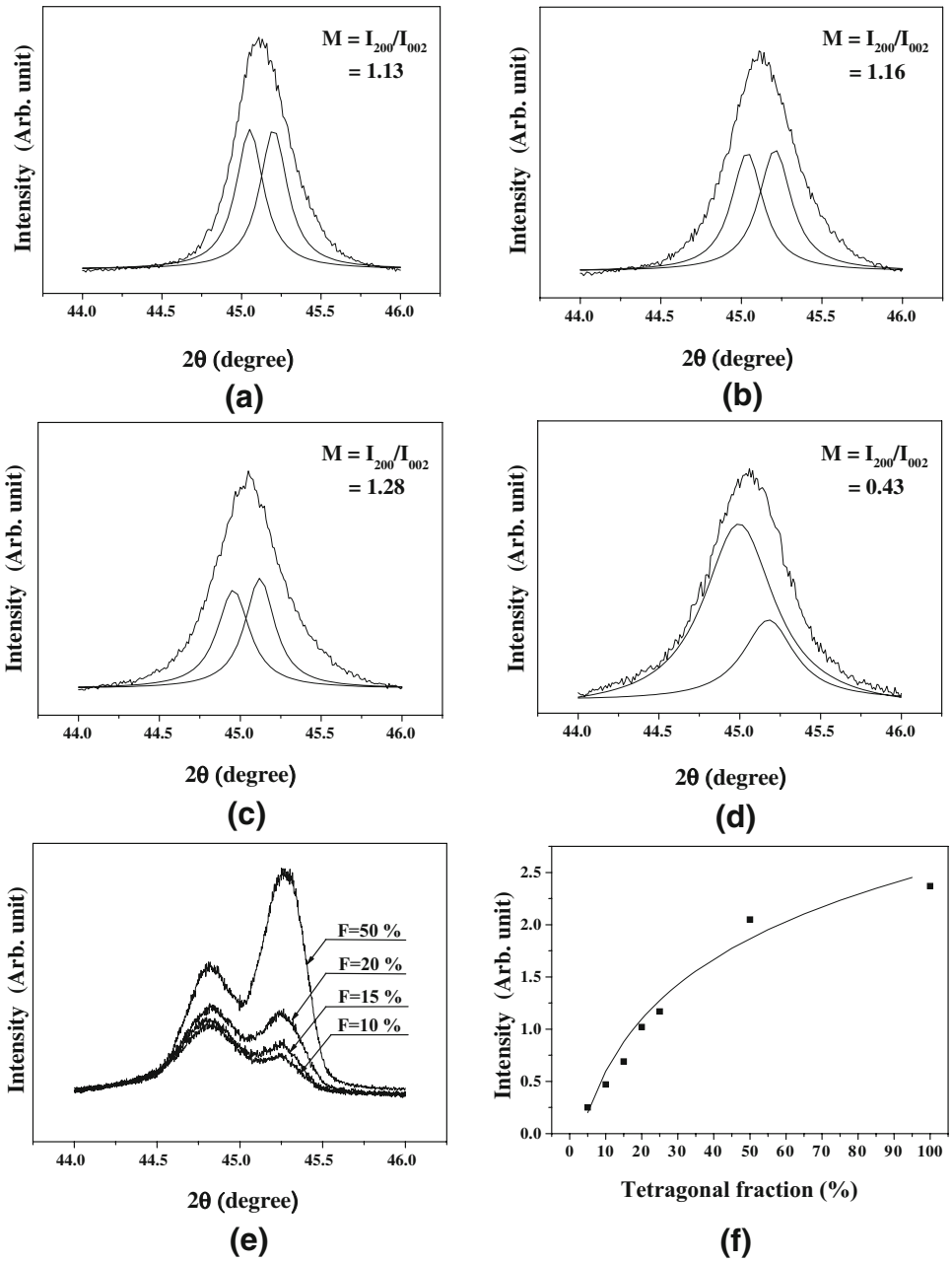

Fig. 3 Spectra in (**a**), (**b**), (**c**), and (**d**) were obtained from the powders prepared at R=1, 0.5, 0.25, and 0.11, respectively; the spectra near 45° were fit with Lorentzian curves corresponding to cubic and tetragonal phases, respectively. (**e**) XRD peaks near 45° were obtained from reference $BaTiO_3$ powder samples; the samples are a mixture of cubic- and tetragonal-phased $BaTiO_3$ powders with known relative volume fraction F [tetragonal/(tetragonal+cubic)] of 10, 15, 20, and 50%. (**f**) Variation in the intensity ratio M, I_{200}/I_{002}, with the known relative tetragonal volume fraction F, tetragonal/tetragonal+cubic, for the reference samples

XRD peaks becomes larger, and such broadening leads to the overlapping of two peaks located close to each other [7]. Because of the peak-broadening, it is difficult to observe separated peaks even when (200) and (002) peaks of the tetragonal phase are expected to exist. Thus, the variation in the relative volume fraction of the tetragonal phase in the nanoscale $BaTiO_3$ powders can be estimated by deconvoluting the overlapped peaks near 45° and applying the intensity relation between (200) and (002) fits.

The observed (200) peaks near 45° were fit with two Lorentzian peaks corresponding to cubic and tetragonal phases [8]. The intensity ratio M, I_{200}/I_{002} was measured to be 1.13, 1.16, 1.28, and 0.43 for the powders prepared at R=1, 0.5, 0.25, and 0.11, respectively. Reference samples with particular amounts of cubic- as well as tetragonal-phased powders were prepared, and then XRD measurements were performed to see the variation in the peaks near 45° with the relative fraction of tetragonal-phased powders; these are shown in Fig. 3 (e). The relation between the ratio M, I_{200}/I_{002}, and known relative volume fraction of tetragonal phases was obtained for powders of F=10, 15, 20, 50, and 100%, respectively. Fig. 3 (f) illustrates the relation can be represented as follows: $M=-1.24+0.78\ln(F)$.

Figure 4 shows the FT-Raman spectra of the samples; spectrum ① obtained from commercially purchased tetragonal-phased $BaTiO_3$ powders are illustrated to be compared with the powders, which were prepared in this experiment at R=0, 0.11, 0.25, 0.5, and 1, respectively; these spectra were recorded in a frequency range of 200~1,400 cm^{-1}, and the peaks near 305 cm^{-1} are illustrated for the comparison of tetragonal phase fraction in the powders. The Raman spectra of all the $BaTiO_3$ powders clearly illustrate the presence of tetragonal phases; the peak at 305 cm^{-1} is seen in all the spectra and their intensity varies depending on R values [9].

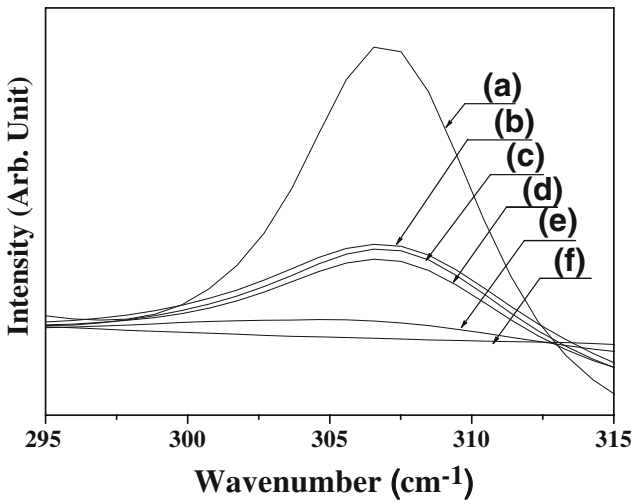

Fig. 4 Raman spectra of the $BaTiO_3$ powders near 305 cm^{-1}. Spectrum (**a**) was obtained from the commercially purchased tetragonal-phased $BaTiO_3$ powders. Spectra (**b**), (**c**), (**d**), (**e**), and (**f**) were recorded from the powders that were prepared at R=0.25, 0.5, 1, 0.11, and 0, respectively

Figure 5 shows the tetragonal fraction for the nanoscale $BaTiO_3$ powders. It seems evident that the cubic and tetragonal phases are present in the powders; the relative fraction of each phase appears to vary depending on the solvent condition R. Fig. 5 (a) was obtained from intensity ratio M (I_{200}/I_{002}) near 45° in the XRD results of Fig. 2; by applying the relationship between M and F seen in Fig. 2 (f), it is clear that the fraction of the tetragonal phases varies from 0 to ~26% as R varies from 0 to 0.25. On the other hand, when R values are 0.5 and 1.0, the tetragonal fractions are ~22 and 20%; these fractions are slightly lower than that of the samples prepared at R=0.25.

In view of the sharp peak at 305 cm^{-1} in the Raman results, it was found that the maximum volume fraction of the tetragonal phase was also obtained when the synthesis was performed at R=0.25. In this analysis, the area under the peak at 305 cm^{-1} was measured to be used for quantitative comparison of the amount of the tetragonal phase; when the powders were prepared at R=0.25, the peak area corresponds to 29% of that of the commercially purchased tetragonal phased $BaTiO_3$.

As a result, the variation in the tetragonal phases obtained from the XRD peak intensity ratio M, I_{200}/I_{002}, with R values seems to agree well with that from the FT-Raman peak ratios at 305 cm^{-1}; the maximum volume fraction of the tetragonal phase was obtained when the synthesis was performed at R=0.25. Such agreement also indicates that both methods can be reliably applicable to the quantitative measurement of the fraction of cubic (or tetragonal) phase in nanoscale $BaTiO_3$ powders.

Figure 6 shows the FT-IR results for the powders. The absorption peak at 1,440 cm^{-1} is due to the asymmetric stretching of the carbonates ($BaCO_3$). The peaks near 1,640

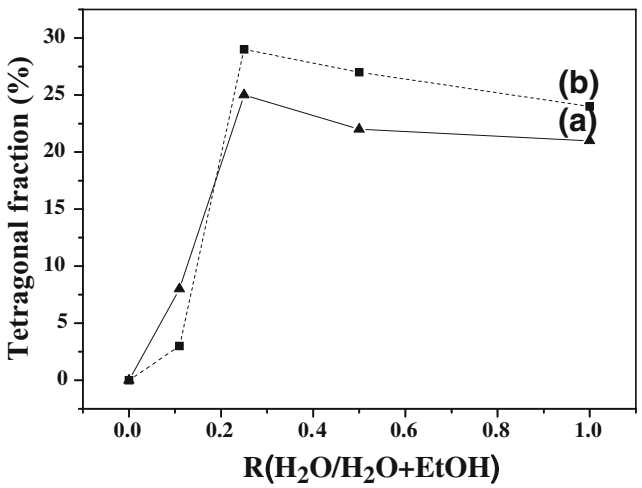

Fig. 5 Variation in the relative tetragonal fraction with R values; curves (**a**) and (**b**) were obtained from XRD and Raman measurements, respectively

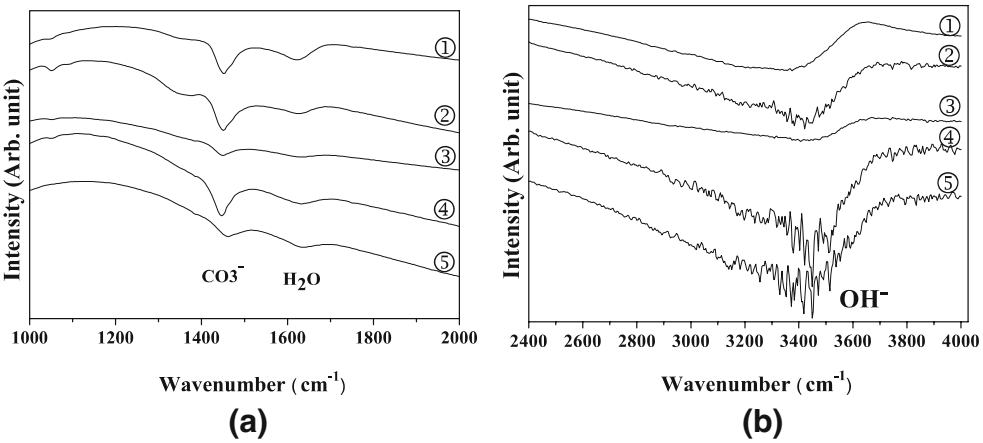

Fig. 6 FT-IR spectra of the $BaTiO_3$ powders. These powders were prepared by hydrothermal synthesis in various solutions at 180°C for 6 h; samples, ①, ②, ③, ④ and ⑤ were recorded from the samples prepared at R=1, 0.5, 0.25, 0.11, and 0, respectively. (**a**) The magnified spectra observed near 1,500 cm^{-1}. (**b**) The magnified spectra observed near 3,400 cm^{-1}

and 3,500 cm^{-1} are associated with the bending mode of H_2O [10]. The FT-IR spectra illustrate that some defects like CO_3^-, OH^-, etc. are present in the crystalline $BaTiO_3$ powders. The intensity of all the absorption bands for these defects significantly decreased at R=0.25. From these results, the defect concentration decreased to be minimized when the powders were prepared at R=0.25. On the other hand, hydroxyl defects are significantly present in the powders prepared at R=0.5; these powders contain ~23% of tetragonal phases.

4 Conclusions

Nanoscale $BaTiO_3$ powders were prepared by hydrothermal techniques, and the phase distribution of the powders was investigated as a function of synthesis solvent conditions. The XRD peak intensity ratio of M, I_{200}/I_{002}, as well as the FT-Raman peaks at frequencies 305 and 710 cm^{-1}, which are sensitive to the presence of tetragonal $BaTiO_3$, indicates that the nanoscale $BaTiO_3$ powders are dominantly of a cubic phase; a relative tetragonal volume fraction of 23~26% is present in the powders prepared at R=0.25~0.5. It was found that XRD and Raman spectroscopy can be reliably utilized in the quantitative analysis of the phase of nanoscale $BaTiO_3$ powders; hydroxyl defects are significantly present in the powders prepared at R=0.5 and 1.0. In our experimental range, R=0.25 is the most suitable condition at which good-quality crystalline $BaTiO_3$ powders with a particular amount of tetragonal phases are synthesized.

Acknowledgement The work was supported by Inha Research Grant 2006.

References

1. M.-B. Park, N.-H. Cho, J. Am. Ceram. Soc. **84**, 1937 (2001)
2. G.A. Smolenskii, V.A. Bokov, V.A. Isupov, N.N. Krainik, R.E. Pasynkov, A.I. Sokolov, Ferroelectrics and Related Materials (Gordon and Breach Science Publishers, New York, London, Paris, Montreux, Tokyo, 1984)
3. B.D. Begg, E.R. Vance, J. Nowotny, J. Am. Ceram. Soc. **77**, 3186 (1994)
4. X. Li, W.H. Shin, J. Am. Ceram. Soc. **80**, 2844 (1997)
5. Y. Kobayashi, A. Nishikata, T. Tanase, M. Konno, J. Electroceram. **29**, 49 (2004)
6. D. Chen, X. Jiao, J. Am. Ceram. Soc. **83**, 2637 (2000)
7. Y. I. Kim, J. K. Jung, K. S. Ryu, Mater. Res. Bull. **39**, 1045 (2004)
8. S.-M. Moon, Chongmu Lee, N.-H. Cho, J. of Electroceram. **17**, 841 (2006)
9. V. Buscaglia, M.T. Buscaglia, M. Viviani, T. Ostapchuk, R. Calderone, C. Harnagea, Z. Zhao, M. Nygren, J. Eur. Ceram. Soc. **25**, 3059 (2005)
10. B.D. Begg, E.R. Vance, R. Nowotny, J. Am. Ceram. Soc. **77**, 3186 (1994)